Earth and Space Science

RESEARCH ARTICLE
10.1029/2018EA000521

Key Points:
- A silver membrane is used to separate oxygen created from a carbon dioxide glow discharge
- This method can be used to generate oxygen from the Martian atmosphere
- Proof of concept experiments validates method of generating pure oxygen from carbon dioxide

Correspondence to:
D. Premathilake,
dvpremathilake@gmail.com

Citation:
Premathilake, D., Outlaw, R. A., Quinlan, R. A., & Byvik, C. E. (2019). Oxygen generation by carbon dioxide glow discharge and separation by permeation through ultrathin silver membranes. *Earth and Space Science*, *6*, 557–564. https://doi.org/10.1029/2018EA000521

Received 15 NOV 2018
Accepted 18 FEB 2019
Accepted article online 18 MAR 2019
Published online 5 APR 2019

Oxygen Generation by Carbon Dioxide Glow Discharge and Separation by Permeation Through Ultrathin Silver Membranes

Dilshan Premathilake[1], Ronald A. Outlaw[1], Ronald A. Quinlan[1], and Charles E. Byvik[2]

[1]Department of Physics, Computer Science and Engineering, Christopher Newport University, Newport News, VA, USA, [2]iPi, Alexandria, Virginia

Abstract A six Torr CO_2 glow discharge in combination with a heated W mesh-reinforced ultrathin Ag membrane is used to generate molecular oxygen. The Ag membrane is a commercially available 25-μm-thick Ag foil backed by a 25-μm-thick W electroformed mesh. The permeation flux is inversely dependent on the membrane thickness and exponentially dependent on the membrane temperature. Calculations show that a pressure differential of 1 atmosphere can be supported by the W mesh/Ag foil membrane at temperatures up to 350 °C. In this work, a glow discharge for pressures between 2 and 15 Torr CO_2 and temperatures up to 500 °C were reported. The DC glow discharge was produced initially with a solid Ag rod cathode, 2 mm in diameter, and then with a 7-mm-diameter Ag rod machined into a hollow cathode, located 5 mm from, and normal to, the Ag membrane anode. The voltage was varied from 440 to 620 VDC with currents up to 41 mA. A stable flux of 1.61×10^{15} O_2 molecules·cm^{-2}·s^{-1} is observed for a membrane temperature of 450 °C and a CO_2 pressure of 6 Torr. With ~4-m^2 surface area, this approach is competitive with the present mission qualified Mars Oxygen In-Situ Resource Utilization Experiment (MOXIE) system planned by National Aeronautics and Space Administration (NASA) for the 2020 Mars rover mission which generates ≈12 g/hr O_2. The proof of concept technique presented herein can be substantially improved by further reduction of the membrane thickness, refinement of the cathode, and glow discharge plasma.

1. Introduction

The NASA Mars 2020 Mission includes the Mars Oxygen ISRU Experiment (MOXIE) to demonstrate producing oxygen from the ~6 Torr CO_2 Martian atmosphere. MOXIE utilizes metal oxide electrodes for the solid oxide electrolysis (Drake, 2009; Hartvigsen et al., 2015; Hartvigsen et al., 2016; Hecht & Hoffman, 2016). A stack of 10 cells, wired in series, produced an O_2 flux of ~12 g/hr. Alternative approaches include CO_2 electrolysis, Sabatier conversion and electrolysis, reverse water gas shift conversion and electrolysis, and glow discharge (Hecht & Hoffman, 2016). The results of glow discharge experiments with reduced Ag membrane thicknesses are reported herein, indicating the potential for scaling this process to be a viable alternative to MOXIE for a Mars Mission.

A DC glow discharge of CO_2 $CO + O$ followed by O permeation through an Ag membrane to generate a high flux of O_2 has been previously reported for membrane thicknesses of 350–400 μm (Outlaw, 1990; Wu et al., 1993, 1996). Oxygen atoms generated by the glow discharge have a high sticking coefficient on the surface of Ag and dissolve rapidly into the octahedral sites of the Ag bulk. This establishes a high oxygen concentration gradient that drives the permeation of oxygen atoms through Ag membrane (Outlaw, 1990; Wu et al., 1993, 1996). This approach is a promising technique for supplying molecular oxygen to support astronaut consumption utilizing the Martian atmosphere (~96% CO_2) on Mars as well as for supplying a propellant constituent for the return trip to earth. To further improve this technique as a viable mechanism for manned Mars missions and colonization, advances must be made that provide sufficient flux density to be cost effective. In past experiments, the Ag membrane thicknesses were machined from Ag castings and ground to thicknesses 350–450 μm, limiting the maximum O_2 flux to ~1×10^{14} cm^{-2} s^{-1}. However, membrane levels below 350 μm will likely result in rupture, even at pressure differentials of ~6 Torr. A significant bulge in the membrane at this pressure difference and at 450 °C has been observed. To mitigate this issue, a 25-μm-thick tungsten electro-formed mesh was sandwiched on the backside (downstream) of a commercially available, pin hole free, 25-μm-thick Ag foil to withstand 5–15 Torr pressure differential at membrane temperature levels >500 °C. The reduction in membrane foil thicknesses to 25 μm is over an order of magnitude

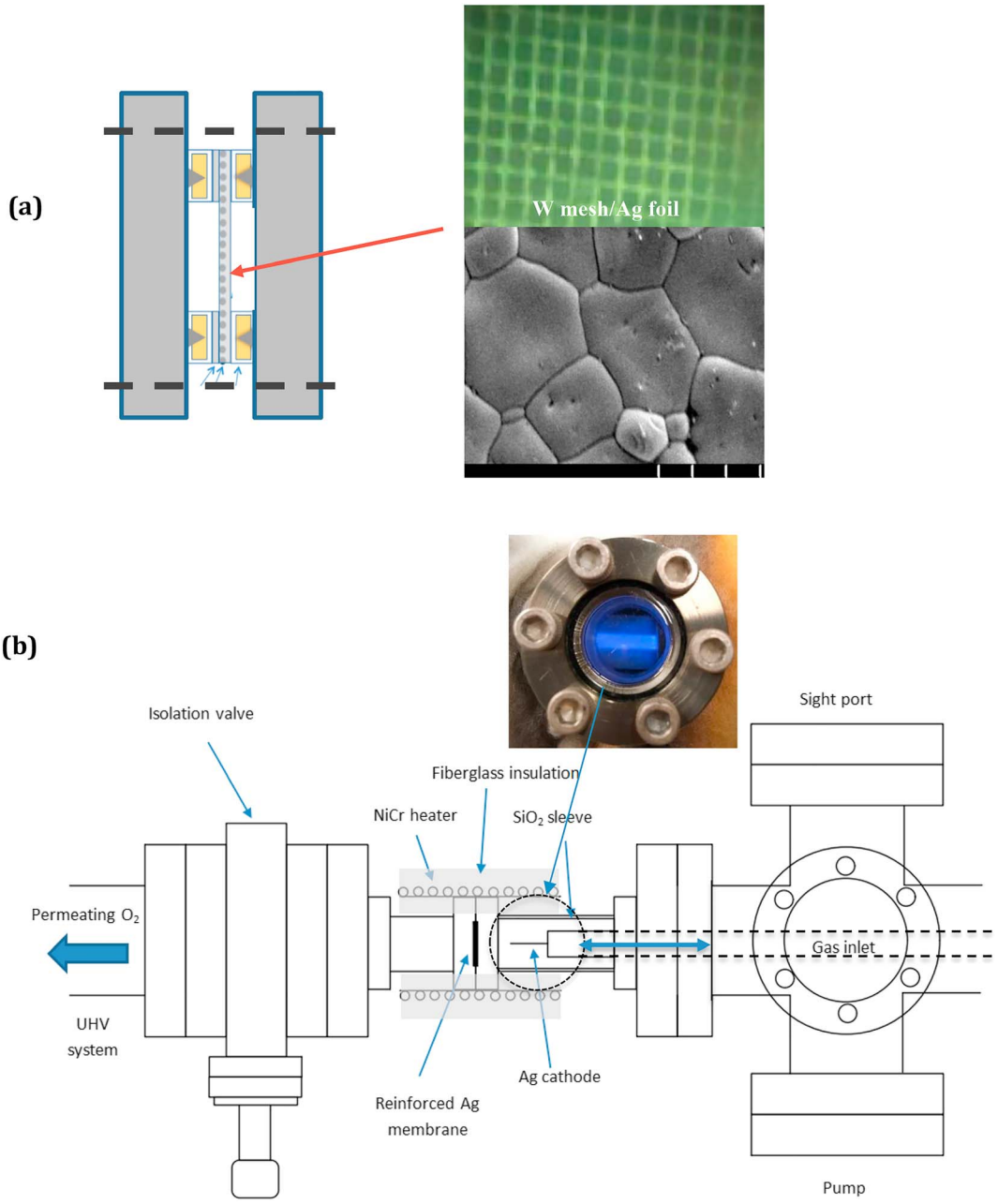

Figure 1. (a) Schematic of the W mesh-reinforced Ag foil cross section compressed between Ag-coated Cu gaskets in miniflange hardware. Optical microscope image of W mesh and an electron microscope image of 25-μm Ag foil is shown on the right (scale is 5 μm per division). Blue arrows point to gaskets and the membrane assembly. (b) Schematic of the glow discharge/permeation system. Inset is a photo of glow discharge observed through the sight port (dashed circle).

thinner than previous work and corresponds to a projected order of magnitude increase in the molecular flux. The primary objective of this work is to show that the CO_2 plasma enhanced permeation of oxygen through Ag is significantly advanced by using W mesh-reinforced thin Ag foils and that this methodology, when developed from proof of concept may be a viable alternative to MOXIE.

2. Experimental

Figure 1a is an optical image of the W mesh-reinforced Ag foil and a scanning electron microscope image of the Ag foil microstructure and a schematic of the assembly compressed between 33.8-mm conflat flange stainless steel hardware (miniflange).

Figure 1b is a schematic of the test system mounted as a radial appendage on the ultra high vacuum (UHV) analysis system. The mesh/foil assembly is separated from the analysis system by an isolation valve. The analysis system is of cylindrical geometry with an in-line quadrupole mass spectrometer for detection of the O_2 flux emanating from the aforementioned W mesh/Ag membrane foil assembly. The ion gauge is mounted adjacent to the mass spectrometer.

The effective oxygen flux transmission area of the membrane assembly is 1.76 cm^2 minus the W mesh area (which reduces the effective emission area of the Ag membrane). The W mesh is 25 μm thick. Optical microscope observations of the mesh show the actual transmission to be 56%. The Ag membrane is 99.99% pure and pin hole free and was tested at a pressure differential of 1 atmosphere. The mesh and foil are sandwiched between two Ag-coated Cu gaskets in the 33.8 mm (1.33″) conflat flange assembly. Initially, an Ag cathode rod of 2 mm in diameter was used and then replaced by a 7-cm Ag rod machined into a hollow cathode tube of 5-mm inner diameter and 10 mm in depth. The cathode is mounted on a linear motion feed through that allows varying the position of the tip from 0 to 10 cm from the upstream membrane surface. In this work, the cathode is positioned 5 mm from the membrane anode. A quartz sleeve lines the tubing over the whole length to insure the discharge is localized at the membrane. The circuit contains a 1 kΩ ballast series resistor. The glow discharge/permeation assembly is a radial appendage mounted on the UHV analysis chamber and separated from the analysis chamber by a gate valve. A 33.8-mm sight port allows observation of the plasma luminescence. The heater for the membrane assembly is beaded nichrome wire wrapped around the W/Ag membrane assembly encompassed in a cylindrical stainless steel sheet to keep the heater coils in a fixed position. A chromel/alumel thermocouple is attached to the periphery of the Ag membrane and the coated Cu gaskets. Fiber glass insulation encompasses the entire heater assembly. The UHV analysis chamber is pumped by an Osaka 1,000 L/s (N_2) magnetically levitated turbo pump, backed by a Pfeiffer turbo/molecular drag 60 L/s (N_2) pumping station. The main chamber above the pump is restricted by a 2″ orifice to conductance limit the analysis region. An SRS 100 mass spectrometer is axially aligned with the glow discharge permeation assembly for detection of the O_2. A UHV nude ion gauge operated at 4-mA emission current is controlled by an SRS model IGC 100 controller to monitor the pressure in the system. The analysis region produces an ultimate pressure of ~5×10^{-10} Torr. The lecture bottle/regulator CO_2 supply is 99.99% pure and is admitted to the upstream region via a precision bleed valve. The pressure in the upstream region is dynamically pumped and kept constant by a Pfeiffer turbo/molecular drag 60 L/s (N_2) pumping station separated from the upstream region by a vacuum valve (slightly open). Control of the upstream pressure is by a UHV bleed valve and pump vacuum valve. This dynamic pumping method insures that CO_2 remains the pure and dominant species (0–15 Torr) in the glow discharge cavity region.

The steady-state oxygen flux permeating through the membrane assembly, $\boldsymbol{J}$, can be represented by

$$\boldsymbol{J}=\boldsymbol{P_{eq}}\boldsymbol{f}/\boldsymbol{AkT}, \tag{1}$$

where $\boldsymbol{P_{eq}}$ is the pressure in the analysis region (i.e., downstream pressure), $\boldsymbol{A}$ is the effective membrane assembly area ($\boldsymbol{A = A_{Ag} - A_W}$), $\boldsymbol{k}$ is Boltzmann's constant, and $\boldsymbol{T}$ is the gas temperature. The constant, $\boldsymbol{f}$, is the effective pumping speed for oxygen through the conductance limited orifice into the turbo pump. The procedure employed is to evacuate both sides of the membrane assembly, establish a membrane temperature, monitor the system mass spectra to insure no leaks, charge the upstream side with CO_2 to the desired pressure (1–15 Torr), apply voltage to initiate the glow discharge strike, set the voltage at the desired level, and then monitor the mass spectra at m/e = 32 in the pressure versus time mode. No thermal dissociative CO_2 adsorption on the Ag followed by oxygen permeation was observed. Following the plasma strike, a rapid increase in the m/e 32 peak was observed. The permeation is concentration gradient driven and, assuming that the surface concentration downstream is zero, the oxygen flux at equilibrium can also can be described by

$$\boldsymbol{J}=\boldsymbol{-DC}/\boldsymbol{d}, \tag{2}$$

where $\boldsymbol{C}$ is the atomic oxygen concentration at the surface, $\boldsymbol{d}$ is the membrane thickness (~25 μm), and $\boldsymbol{D}$ is the diffusion coefficient of atomic oxygen through Ag, ($\boldsymbol{D} = 3.2 \times 10^{-2}\exp[-15{,}330/\mathrm{RT}]$ cm^2/s). Combining

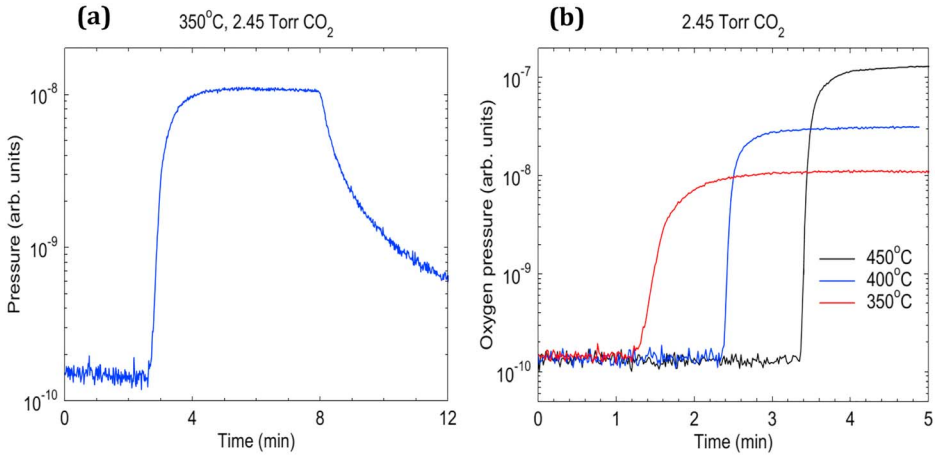

Figure 2. (a) CO_2 glow discharge-enhanced permeation of the oxygen flux detected downstream in the analysis chamber at 350 °C, at strike and at voltage termination. (b) Plasma strike at 350, 400, and 450 °C. The baseline of the strike curves has been adjusted to the same thermal oxygen level for the three temperatures of the Ag.

equations (1) and (2) allows calculation of the surface concentration for temperature conditions less than 600 °C.

$$\boldsymbol{C}=(\boldsymbol{P_{eq}}\,\boldsymbol{f}\,\boldsymbol{d})/(\boldsymbol{DAkT}). \tag{3}$$

At 450 °C and $\boldsymbol{P_{eq}} = 2.73 \times 10^{-7}$ Torr CO_2 downstream pressure (6 Torr (CO_2) upstream), the O_2 flux ($\boldsymbol{J}$) is 1.61×10^{15} cm^{-2} s^{-1}, corresponding to a surface concentration, $C_s = 2 \times 10^{18}$ atoms per cm^3. Since the number of adsorption sites on a perfect crystal of the Ag surface is ~10^{15} cm^{-2}, this anomaly can be explained, in part, by the value of D. The value used in this calculation is for volume (lattice) diffusion of oxygen through large grain Ag ($\delta > 1$ mm; Outlaw & Sankaran, 1988). In the work of Hoffman and Turnbull, comparing the self-diffusion in large-grain and small-grain Ag (δ~35 μm), they found a difference >10^3 because of dominant grain boundary diffusion (Hoffman & Turnbull, 1951). In this work, grain boundary diffusion is clearly the mechanism since the average grain size, $\delta \sim 15$ μm. See Figure 1a. The sticking coefficient of O_2 on Ag is very low (~10^{-3} on the (110) face and ~10^{-6} on the (111) face), but the oxygen atom adsorption on the (110) face is ~1 (Campbell, 1985; Engelhardt & Menzel, 1976). This suggests that the concentration of oxygen atoms on the upstream surface is very high, but the permeation is still limited by grain boundary diffusion because it increases with temperature and exhibits a linear Arrhenius behavior.

3. Results and Discussion

Figure 2 shows the change in O_2 flux as a function of time for a membrane temperature of 350 °C and a strike voltage of 480 VDC. Since there is only a slight permeation at 250 °C and a modest permeation at 300 °C, this work is limited to 350 °C and above. O atoms and O* excited states are the predominant adsorbed species at the anode since O+ ions areSince there is only a slight forbidden. The curves in Figure 2 are for an initially depleted bulk oxygen concentration in the Ag membrane indicating that it takes longer to reach equilibrium. At 350 °C, the signal rises almost two orders of magnitude and reaches equilibrium within 2 min. Figure 2b shows the plasma strike rise for membrane temperatures of 350, 400, and 450 °C. The baseline has been adjusted to the same O_2 permeation signal magnitude for comparison. The decay rate of the O_2 signal after the strike is terminated is a function of the oxygen concentration in the Ag bulk at the time of plasma termination. In Figure 2a, the solubility of O/Ag was minimal, so the signal dropped rapidly. After achieving steady state for times, $t > 10$ min, the oxygen desorption slowed noticeably indicating a slight bulk diffusion limited permeation. When the upstream CO_2 was pumped away, the m/e = 32 amu rapidly decayed to the original main chamber background (pumping on both sides of membrane).

Figure 3 is mass spectra of background during glow discharge strike at 450 °C. Note the substantial increase in fragmentation peak at m/e = 16 amu and parent peak O_2 at m/e = 32 amu. An increase in CO_2 was also

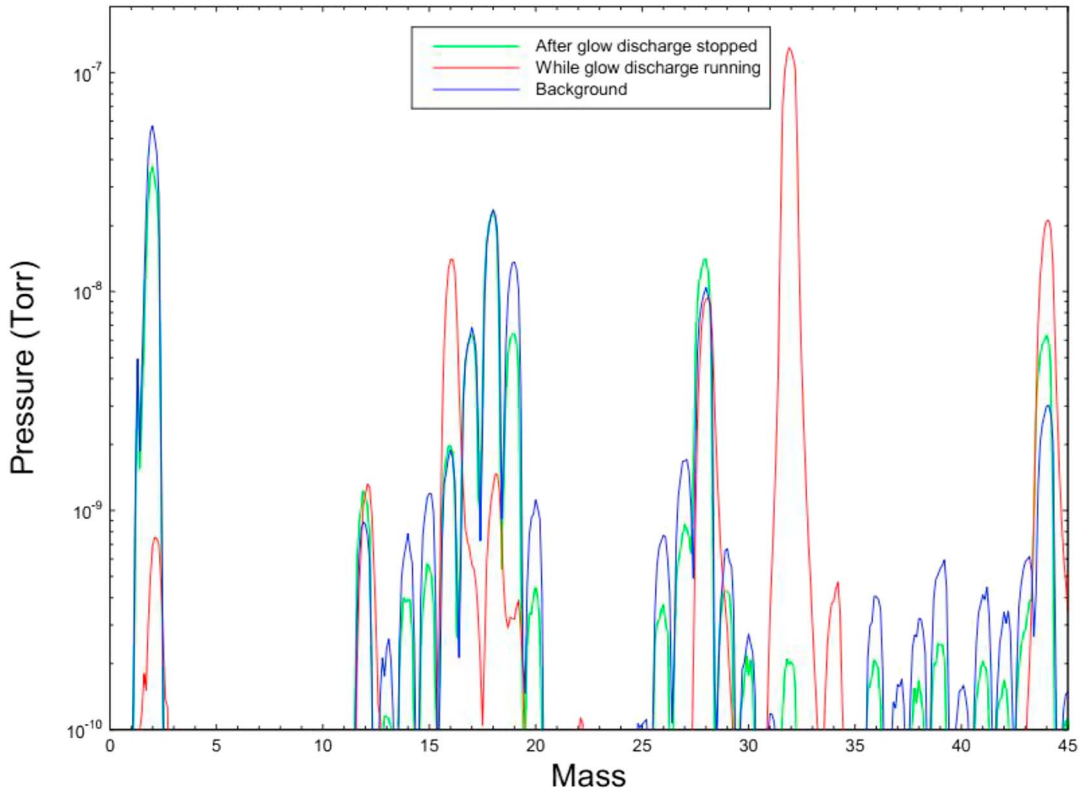

Figure 3. Mass spectra of the analysis system before (blue), during (red), and after glow discharge (green). No significant O_2 existed before the glow discharge, but it dominated all species during the discharge.

observed because of the reaction of the inordinately high increase in O_2 reacting with surface adventitious carbon in the analysis chamber that exists on virtually all the system surfaces. No significant increase in CO (m/e = 28) was observed. Molecular scrubbing was also observed, ultimately resulting in a reduction in all outgassing species in the system, particular H_2O. A small increase in hydrogen peroxide (m/e = 34) occurred during the glow discharge but disappeared immediately following a termination of the voltage.

The flux rise to a steady-state condition is more rapid than at 350 °C (~45 s). At steady state, the voltage was increased in 10-V increments to 620 V. Figure 4 is a typical strike at 400 °C, 2.45 Torr of CO_2. The flux rise to steady state is more rapid giving a staircase signal with the O_2 flux increasing by a factor of 7. Note that the curve shown in Figure 4b is smooth and monotonically increasing suggesting the increased voltage increases the plasma energy promoting more O atoms arriving at the upstream surface. The current varied from 2 mA at 480 V to 4 mA at 620 V. A factor of 2 increase in signal was observed when the cathode was temporarily moved to 2 mm from the anode, resulting in compression of the positive column and a greater density of neutral O atoms nearer to the anode (Raizer, 1987).

Figure 4c is O_2 flux ($\boldsymbol{J}$) versus time data taken with the Ag hollow cathode (7-mm diameter with a concentric machined opening of 5 mm in diameter and 10 mm deep), located 5 mm from the membrane anode. The membrane temperature was 450 °C with an upstream pressure of 6 Torr (CO_2) and a voltage of 509 V. At this voltage, 41-mA current was observed.

The hollow cathode showed more stability than the solid rod used previously (Mavrodineanu, 1984; Rossnagel, 1991). Additional runs eventually gave a steady downstream analysis chamber pressure more than three orders of magnitude to 2.73×10^{-7} Torr (O_2) which, from equation (1), is equivalent to $\boldsymbol{J} \sim 1.61 \times 10^{15}$ cm^{-2} s^{-1}. The small oscillation during the glow discharge is a result of the difficulty in manually maintaining the upstream pressure at a constant 6 Torr (CO_2) and maintaining the Ag membrane at 450 °C. The plasma strike further heats the membrane and increases the temperature by ~15 °C. When the voltage was turned off, the pressure immediately decreased and continued to decline via bulk thermal desorption.

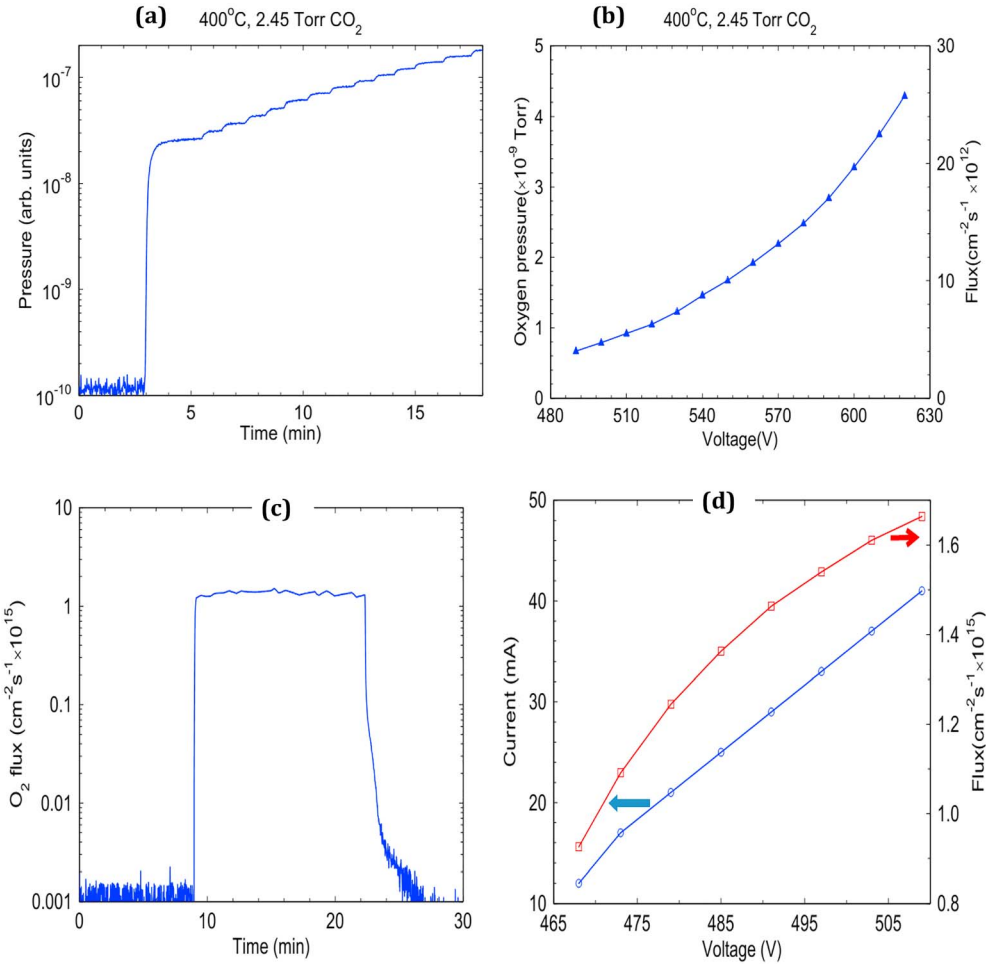

Figure 4. (a) Plasma strike at 400 °C, 2.45 Torr CO_2, and 480 V. The rise is over two orders of magnitude in less than 1 min. After reaching steady state, the voltage was increased in 10-V increments. (b) Molecular oxygen pressure and flux as a function of staircase voltage in (a). (c) Downstream O_2 flux versus time plot at 450 °C, 6 Torr (CO_2), 509 V, and 41-mA plasma. (d) O_2 flux (red) and plasma current versus plasma voltage.

When the upstream CO_2 was pumped away, the pressure continued to rapidly decline as the bulk oxygen thermally desorbed from both sides of the membrane. During the strike, in addition to the Ag membrane, the observed plasma covered a stainless steel region of >35 cm^2 concentrically located around the cathode (as observed through the sight port). Thus, confining the plasma to 1.76-cm^2 Ag membrane area would substantially reduce the power required. Data were taken at CO_2 pressures up to 15 Torr with corresponding increases in the downstream system pressure up to 9×10^{-7} Torr and a corresponding increase of the O_2 flux by a factor of 5.6 but, although interesting, is beyond the atmospheric pressure on Mars.

Since permeation is a function of 1/d, the glow discharge enhanced permeation through a 25-μm Ag foil should be significantly greater than previously reported for membranes of 350- to 400-μm thickness. Wu et al. (1996) reported a flux of ~1.0×10^{14} cm^{-2} s^{-1} for a 350-μm-thick Ag membrane at 450 °C and 5 Torr (CO_2) at 2.5-mm cathode-anode separation. Therefore, for this membrane which is 14× thinner, the flux is expected to be a factor of 14× greater under the same conditions. Wu et al. (1996) used a similar Ag hollow cathode but was 2.5 mm from the membrane anode, thus observing a factor of two greater flux than at 5 mm. At 450 °C and an applied voltage of 550 V (actual plasma voltage 509 V accounting for the voltage drop across the series ballast resistor), we have achieved analysis chamber pressures of 2.73×10^{-7} Torr (O_2) which corresponds to O_2 flux levels of 1.61×10^{15} cm^{-2} s^{-1}(O_2). Figure 4d shows the variation of plasma current and the downstream pressure versus plasma voltage. Plasma strike was stable down to 440 V, at which time it

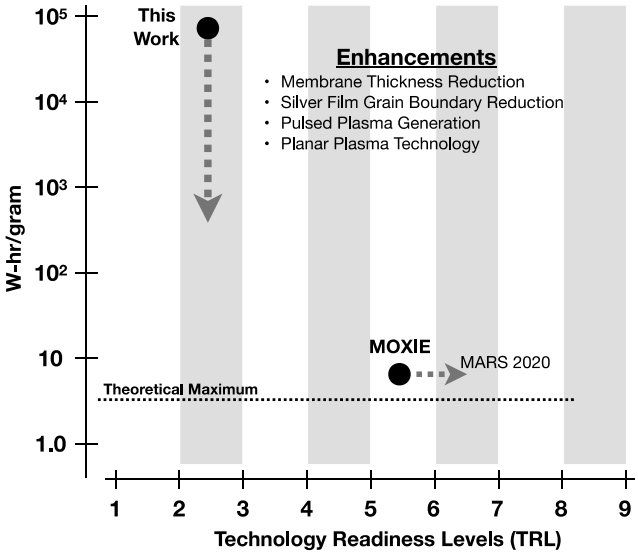

Figure 5. TRL for glow discharge proof of concept experiment and Mars Oxygen ISRU Experiment (MOXIE) corresponding power conversion efficiencies.

extinguished. The apparent linearity of the plasma current as a function of voltage differs from the nonlinearity observed in Figure 4b. This is attributed to the greater stability of the hollow cathode compared to the solid rod cathode. The results shown indicate a flux of ~3.1×10^{-4} g·cm^{-2}·hr^{-1}.

MOXIE is the state-of-the art for converting the CO_2 atmosphere on Mars to O_2. The significant development and testing of MOXIE to optimize performance for operation in the Martian atmosphere for the Mars 2020 Mission suggests a Technology Readiness Levels (TRL) of 5–6. Following successful operation on Mars, the TRL will advance to TRL 6–7. Its 10 cells in series operating at 800 °C is expected to convert compressed CO_2 at a rate of 10 g/hr for 60-W input power resulting in a power conversion efficiency of 6 W·hr^{-1}·g^{-1}. The theoretical maximum power conversion efficiency at thermoneutral voltage of 1.46 V is 4.9 W·hr^{-1}·g^{-1}.

The generation of oxygen by glow discharge and separation by ultrathin silver membranes reported in this work is a proof of concept and meets the criteria for TRL 2–3. Figure 5 illustrates the TRL and performance of these two techniques. The power conversion efficiency for glow discharge in this effort is ~9.9×10^4 W·hr^{-1}·g^{-1}. Although there are orders of magnitude difference in the power efficiencies of a proof of concept experiment compared to the theoretical maximum and MOXIE, there are a number of feasible technical improvements that can be made to enhance, by orders of magnitude, the viability of the glow-discharge approach for the Mars mission. These include (a) reducing membrane thicknesses another order of magnitude using W mesh-reinforced Ag foils 2.5 μm thick, (b) microporous substrates on which a pin hole free thin film of Ag would serve as the membrane (<1-μm thickness), (c) adapting planar plasma glow discharge technology for reductions in voltage enabled by micrometer-scale electrode gaps (Go & Pohlman, 2010), and (d) exploring pulsed power plasma techniques under development at the University of Lisbon. Pulsed power plasmas will be applicable to this approach to further reduce the energy budget (Guerra et al., 2017). Pulse widths 5 ms on and off to create plasmas that are more efficient in dissociating CO_2 have been reported (Silva et al., 2017).

4. Summary

The use of commercially available pin hole free 25-μm Ag foils reinforced by an electroformed W mesh to prevent rupture under a differential pressure of six Torr CO_2 allowed more than a factor of 10 increase in oxygen permeation flux compared to previous experiments with machined ~350–400-μm Ag membranes. This work shows that 25-μm-thick pin hole free Ag foils can be adequately supported by 25-μm-thick electroformed W mesh at pressure differentials of 1 atmosphere for room temperatures up to 350 °C. We have observed downstream analysis chamber pressures of 2.73×10^{-7} Torr (O_2) which corresponds to O_2 flux levels of 1.61×10^{15} cm^{-2} s^{-1}(O_2). In this present state of development, a 4-m^2 area would be required to yield MOXIE O_2 flux levels of ~12 g·cm^{-2}·hr^{-1} MOXIE, and its considerable development and testing have resulted in a package for the Mars Rover that provides an important baseline of quantified operational performance parameters including power, mass, volume, efficiency, and risk to assess viability of alternative technology approaches. This paper provides results of the glow discharge technology for In-situ resource utilization (ISRU) generation of oxygen and is offered as a technology risk reduction approach for the Human to Mars Mission.

Acknowledgments
The authors would like to thank G. Mulvey of the University of the Incarnate Word for his observation of the initial work at the University of Lisbon, Department of Physics, on glow discharge plasma dissociation of CO_2 and their promotion of the technique being competitive to the MOXIE work at MIT (Rossnagel, 1991). All data obtained in conducting this research have been included in the manuscript text and figures.

References

Campbell, C. T. (1985). Atomic and molecular oxygen adsorption on Ag(111). *Surface Science*, *157*(1), 43–60. https://doi.org/10.1016/0039-6028(85)90634-X

Drake, B. G. (2009). Human Exploration of Mars, Design Reference Architecture 5.0, NASA SP 2009 566.

Engelhardt, H. A., & Menzel, D. (1976). Adsorption of oxygen on silver single crystal surfaces. *Surface Science*, *157*(2), 591–618.

Go, D. B., & Pohlman, D. A. (2010). A mathematical model of the modified Paschen's curve for breakdown in microscale gaps. *Journal of Applied Physics*, *107*(10), 103303. https://doi.org/10.1063/1.3380855

Guerra, V., Silva, T., Ogloblina, P., Grofulovic, M., Terraz, L., Sa Silva, M., et al. (2017). "The case for in situ resource utilization for oxygen production on Mars by non-equilibrium plasmas". *Plasma Sources Science and Technology*, *26*(11). https://doi.org/10.1088/1361-6595/aa8dcc

Hartvigsen, J., Elangovan, S., Elwell, J., Larsen, D., & Clark, L. (2016). 12th European SOFC and SOE Forum, paper A1403.

Hartvigsen, J., Elangovan, S., Larsen, D., Elwell, J., Bokil, M., Frost, L., & Clark, L. (2015). Challenges of solid oxide electrolysis for product of fuel and oxygen from Mars atmospheric CO_2. *SOFC-XIV, ECS Transactions*, *68*(1), 3563–3583. https://doi.org/10.1149/06801.3563ecst

Hecht M., & Hoffman X. (2016). "The Mars Oxygen ISRU Experiment (MOXIE) on the Mars 2020 Rover", 3rd International Workshop on Instrumentation for Planetary Missions.

Hoffman, R. E., & Turnbull, D. J. J. (1951). "Lattice and grain boundary self-diffusion in silver". *Applied Physics*, *22*(5), 634–639. https://doi.org/10.1063/1.1700021

Mavrodineanu, R. (1984). "Hollow cathode discharges—Analytical applications". *Journal of Research of the National Bureau of Standards*, *89*(2), 147.

Outlaw, R. A. (1990). O_2 and CO_2 glow-discharge assisted oxygen transport through Ag. *Journal of Applied Physics*, *68*(3), 1002–1004. https://doi.org/10.1063/1.346734

Outlaw, R. A., & Sankaran, S. N. (1988). Oxygen transport through high purity, large grain Ag. *Journal of Materials Research*, *3*(06), 1378–1384. https://doi.org/10.1557/JMR.1988.1378

Raizer, Y. P. (1987). *Gas discharge physics*, (p. 170). New York: Springer.

Rossnagel, S. N. (1991). "Glow discharge plasma and sources for etching and deposition", *Thin film processes*. San Diego, CA: Academic Press, Inc.

Silva T., Grofulovic M., Klarenaar B. L. M., Guaitella O., Engeln R., Pintassilgo C. D., & Guerra V. (2017). "Understanding the electron and vibrational kinetics in CO2 plasmas", Proceedings of the ICPIG XXXIII (International Conference on Phenomena in Ionized Gases) Portugal Estoril.

Wu, D., Outlaw, R. A., & Ash, R. L. (1993). Glow discharge enhanced permeation of oxygen through silver. *Journal of Applied Physics*, *74*(8), 4990–4994. https://doi.org/10.1063/1.354304

Wu, D., Outlaw, R. A., & Ash, R. L. (1996). Extraction of oxygen from CO_2 using glow-discharge and permeation techniques. *Journal of Vacuum Science and Technology A*, *14*(2), 408–414. https://doi.org/10.1116/1.580098